A Low-Cost Altitude Control System for the Kadet Senior Radio-Controlled Airplane

Angel Abusleme, *Member, IEEE*, Aldo Cipriano, *Senior Member, IEEE*, and Marcello Guarini

***Abstract*—In automatic control education, real examples always improve students' learning and motivation. Considering this fact, a hardware-in-the-loop, low-cost altitude control system for a radio-controlled (RC) airplane has been developed to improve automatic control education. This system constitutes a high-impact demonstrator for teaching automatic control topics, applied to a real-life problem. The airplane has an altitude sensor; students can safely remotely control this variable in a computer real-time environment. This paper addresses the system analysis and description, controller design, and real demonstrations. This device was tested in a basic automatic control course for undergraduate electrical engineering students and received good results; students reacted with curiosity and enthusiasm and encouraged the lecturers to design more experiences like this one.**

***Index Terms*—Automatic control education, longitudinal control, proportional-integral-derivative (PID) control, unmanned air vehicles, Ziegler–Nichols tuning method.**

I. Introduction

AUTOMATIC control education can be improved by using high-impact demonstrators, such as ball-and-beam systems or inverted pendulum and magnetic levitation systems [1], [2]. Students show interest and motivation for these systems and can apply their knowledge about most automatic control topics in a real system. With this idea, a low-cost altitude control system for an remote-controlled airplane was designed and developed to improve teaching on automatic control topics for undergraduate electrical engineering students.

The system—an experimental platform—consists of a radio-controlled (RC) airplane with speed and altitude sensors on board, a communications module, and a ground control computer, as shown in Fig. 1. (Although both speed and altitude can be controlled, this paper only addresses the altitude control.) This hardware-in-the-loop platform lets students test their control algorithms, previously developed by simulation, in a highly nonlinear dynamic system. Students may change the control algorithm by just replacing one block in a Simulink environment. This device is also a high-impact and motivating demonstrator, making the platform highly recommendable as a teaching device for automatic control courses.

The Sig Kadet Senior RC airplane was chosen because of its inherent stability, high storage capacity, and low cost. Some parts of the airplane were modified to provide more room internally for all the electronic equipment. An altitude sensor, designed and implemented by the authors to reduce costs, was mounted on the airplane. An RF communications module was also implemented to send sensor data to a ground computer, which processes the information and generates the manipulated variables to control the airplane. This information is sent to the airplane using a standard RC transmitter. The lateral dynamics of the airplane are manually controlled using a standard joystick connected to the computer. The block diagram of this system just presented is shown in Fig. 1. The control algorithms for the longitudinal dynamics (speed and altitude) may be tested using a simulator based on the mathematical model of the airplane.

Section II describes the experimental platform, including the altitude sensor and communication systems, and Section III presents the mathematical model of the airplane and control strategies developed to test the system. Finally, real tests and demonstrations are described and discussed.

Manuscript received October 31, 2001; revised April 7, 2002. Project 1990101 was supported by the Fondo Nacional de Desarrollo Cientifico y Tecnológico (FONDECYT) under Project No. 1990101.

The authors are with the Pontificia Universidad Católica de Chile, Correo 22, Santiago, Chile.

Digital Object Identifier 10.1109/TE.2002.804413

II. Experimental Platform

The basic platform consists of the airplane, an altitude sensor (the speed sensor will not be considered in this paper), communication and acquisition systems, and a ground computer. This section describes these components and how they are connected.

A. Kadet Senior Airplane

The Kadet Senior (shown in Fig. 2) is a 4-kg-weight RC airplane manufactured by Sig, with a 1.98-m wingspan, which is large enough to lift the electronic equipment; during tests, it was loaded with approximately 2 kg of extra weight, with no major problems for flying. It is also inherently very stable and flies at low speeds. It cannot perform aerobatics or complex maneuvers because it is designed to fly smoothly: it has an elevated dihedral angle, flat-bottomed airfoil high-wing structure. These features make the Kadet Senior an appropriate model for testing control algorithms for longitudinal dynamics.

B. Altitude Sensor

This sensor was designed to measure the airplane's altitude from 0 to 70 m with high resolution (at least 8 b), excellent dynamic response, and low cost. The airplane altitude was determined by measuring the barometric pressure using a Motorola MPX4100AP micromachined absolute pressure sensor, with a 0–105-kPa range. The sensor output was signal-conditioned using opamps and calibrated with a start-up sequence programmed in a PIC16F876 microcontroller. This routine sets the zero-altitude limit for the current atmospheric

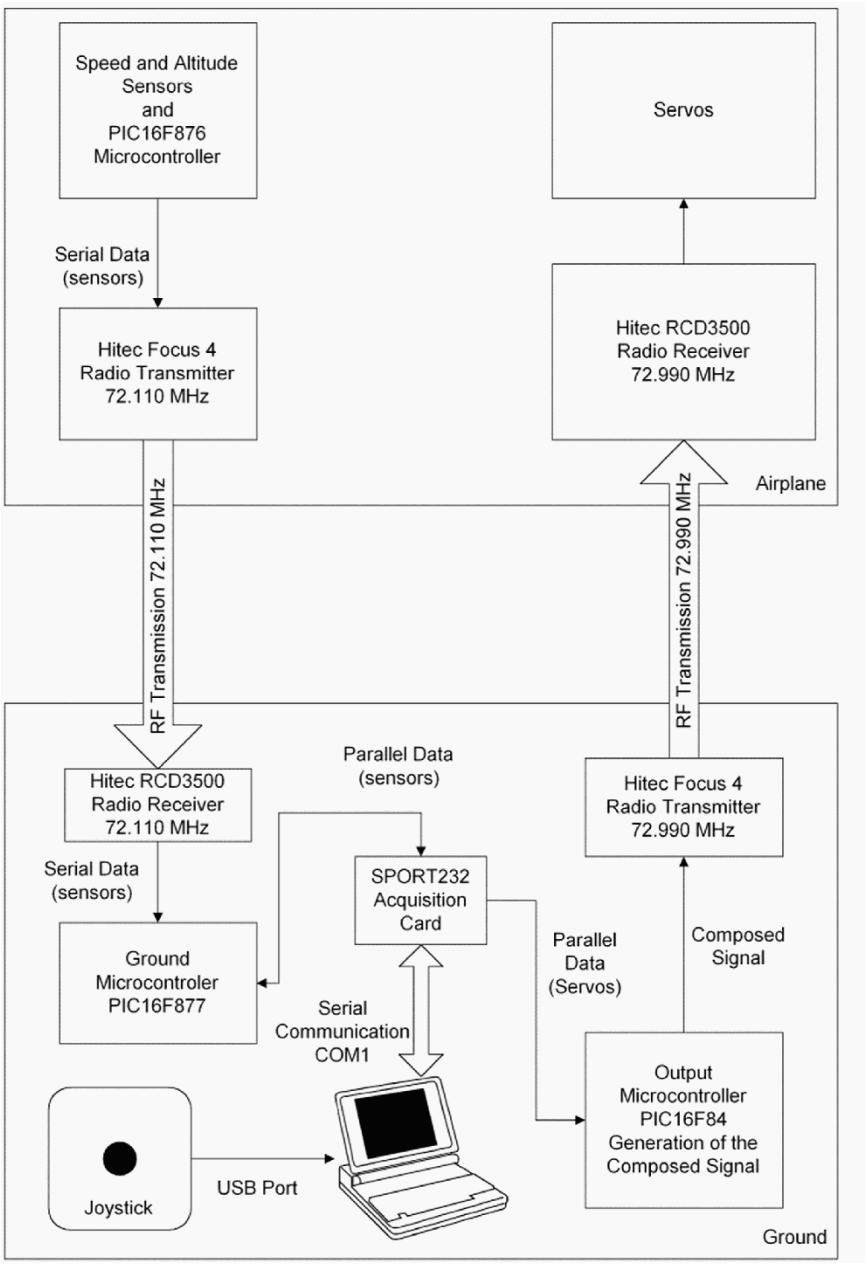

Fig. 1. Block diagram for the experimental platform.

pressure. The output of this sensor, shown in Fig. 3, is sampled using one of the microcontroller 10-b A/D converters.

The sensor was tested and calibrated in a high building, whose altitude was already established. The sensor proved to be sensitive enough to respond to changes in altitude of 0.3 m. The sensor can measure complete flights of the airplane, generating the nonfiltered curve shown in Fig. 4. This curve demonstrates sensor quality and sensitivity and its ability to provide the information necessary to control the airplane. Sensor circuits (shown in Fig. 5) are mounted in the wing next to the Pitot tube and send serial data packets to the RF transmitter using a cable. Because of the signal-conditioning circuits, the sensor responds as a first-order system with a time constant of 0.03 s.

The airplane climb rate can be directly derived from altitude measurements. However, this signal is too noisy and dif-

Fig. 2. The Kadet Senior Airplane.

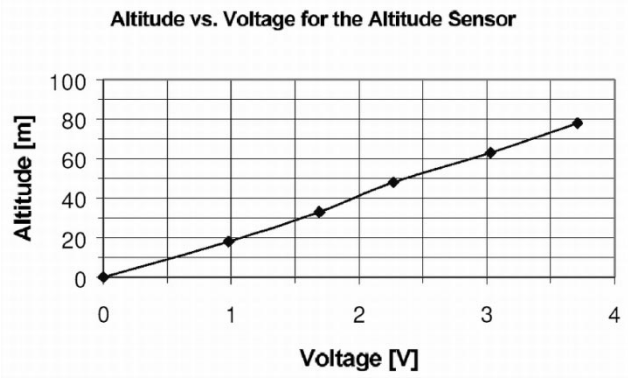

Fig. 3. Relationship between altitude and output voltage for the altitude sensor.

ficult to handle; the high-frequency components generate noisy responses from the proportional integral derivative (PID) controller. To avoid this problem during the real control of the airplane, the climb rate was obtained using the approximate derivative of the altitude and filtering high-frequency components.

C. Communication and Acquisition Systems

The purpose of the communications module is to transmit sensor data to the ground computer and manipulated variables to the airplane's servos. To achieve the first objective, the microcontroller on the airplane sends serial data packets to the Hitec Focus 4 RF transmitter at 1 kb/s. Each packet has 1 initial b, 2 address b, and 10 data b/sensor. The information is sent to the Hitec RCD3500 RF receiver on the ground (maximum distance: 1 km). Serial packets are decoded and stored in the PIC16F877 ground microcontroller. This microcontroller also communicates the information from each sensor to the ground computer through a parallel bus connected to the SPORT232 acquisition card, which sends data to the PC via an RS232 serial port. These actions happen every time the computer requires new data (0.1 s).

The computer works in a MATLAB environment using Simulink. All the routines (including the controllers, the serial transmission/reception (Tx/Rx) routines required to communicate between the computer, and the SPORT232 acquisition card) are easily programmed with MATLAB libraries and C++ language. This programming lets users change any controller by replacing a single block in the Simulink model, making it easier for students to test different control systems without modifying the entire model.

The manipulated variables are generated in the computer and sent through the data acquisition card to another microcontroller (PIC16F84), generating the composed signal, which is then sent to the RC transmitter. The Hitec radio transmitter interprets that signal as a standard RC signal, so the airplane cannot determine whether the controller is the computer or a human pilot.

To avoid any signal interference, the airplane receiver was placed as far as possible from the transmitter (1 m, with the antennas extended at a right angle). This placement ensures the excellent performance of duplex communications system within the airplane's flying range.

The experimental platform costs $1000 (for the airplane, engine, communication systems, sensors, and acquisition and interface cards) and was developed in one year. Obviously, this cost does not represent the development cost (i.e., design time, testing of different sensors and communication systems, airplane crashes, and repair costs, etc.).

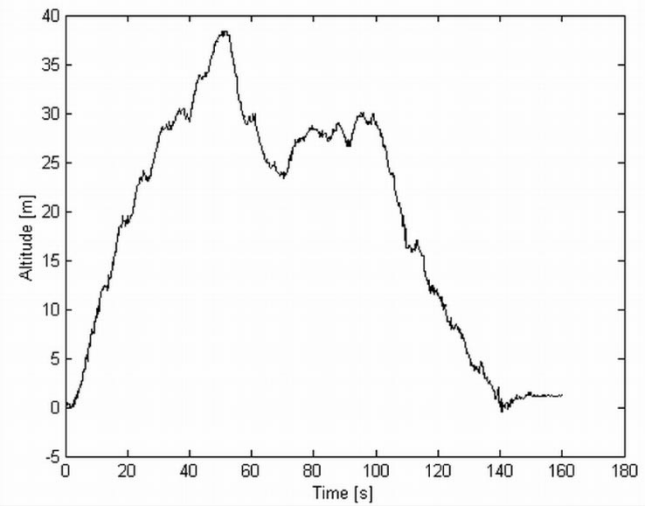

Fig. 4. Altitude measurements during a flight.

III. Model Simulator

The numerical parameters of most standard mathematical models for airplanes are usually obtained from wind tunnel test results using a scale model [3], [5]. These models are evaluated at each operating point using information obtained during tests. More sophisticated nonlinear models approximate aerodynamic coefficients using a truncated Taylor series [6]. They also need wind tunnel tests to obtain those curves.

This paper describes a phenomenological generic model that uses parameters obtained from the physical characteristics of the Kadet Senior airplane. The block diagram of the model is shown in Fig. 6.

The model consists of three highly coupled, nonlinear differential equations, most of whose terms are aerodynamic forces. The manipulated variables are the elevator angle δ_e and the engine duty cycle δ_T. Both variables influence the airplane's angular Q, longitudinal U_A, and transversal W_A speed. By applying a coordinate transformation to these three variables, the airplane's horizontal speed V_X and vertical speed V_Z on the ground reference system are obtained.

Each of the forces acting on every surface of the airplane depends nonlinearly on the total speed V_T, angle of attack α, the manipulated variables δ_e and δ_T, the altitude, the air density, the aerodynamic coefficients for the surface, etc. This dependence is expressed as a nonlinear function, which is approximated to reduce programming costs.

Model simulation tests were executed for changes in both manipulated variables. Results, not included in this work, were compared with those generated by the same tests on the real airplane and showed that the model response is qualitatively similar to the airplane's real behavior. However, there were some important differences regarding the airplane's sensitivity to changes in the elevator angle. These differences were corrected in the latest version of the model by changing the

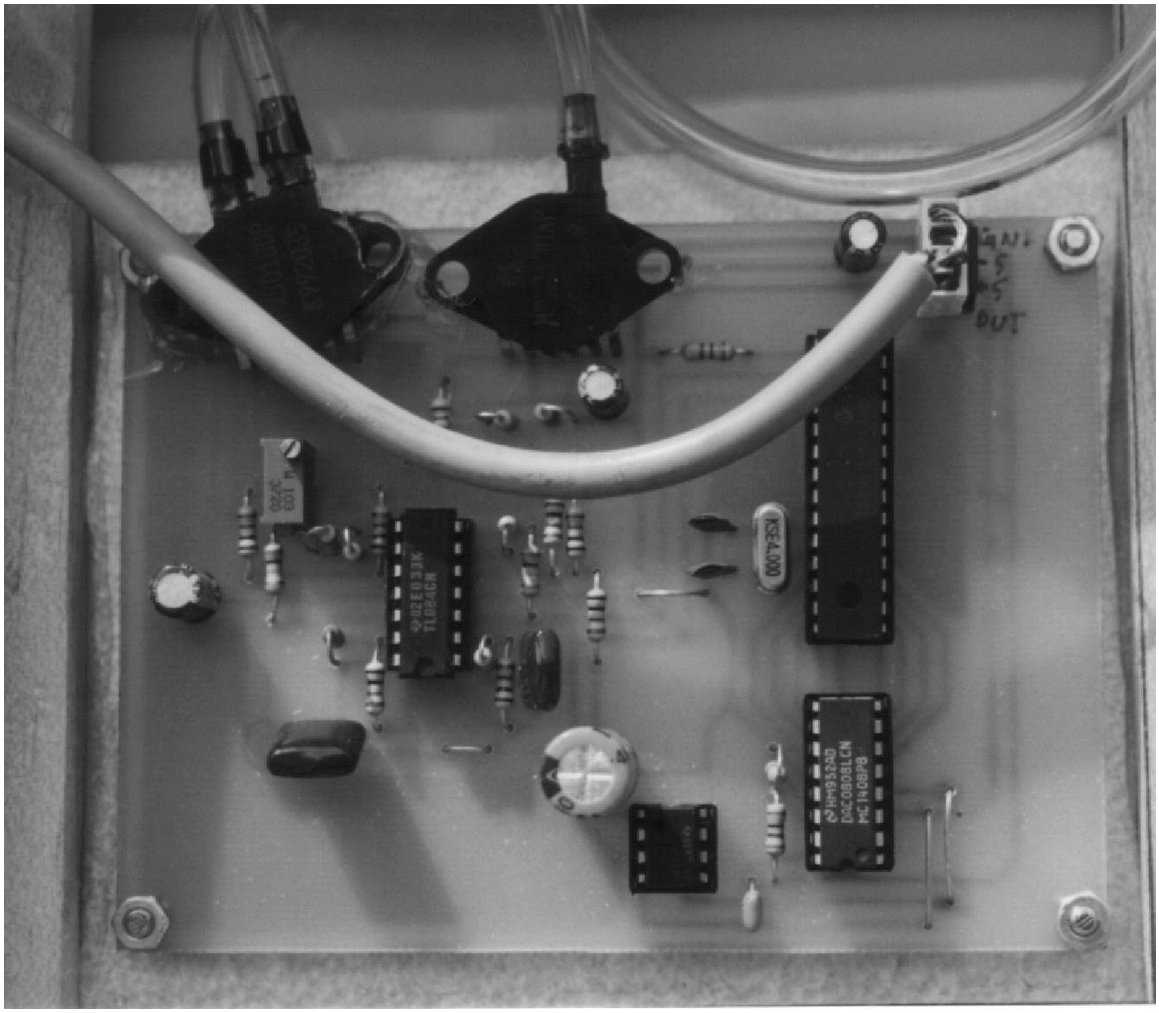

Fig. 5. Altitude measurement card.

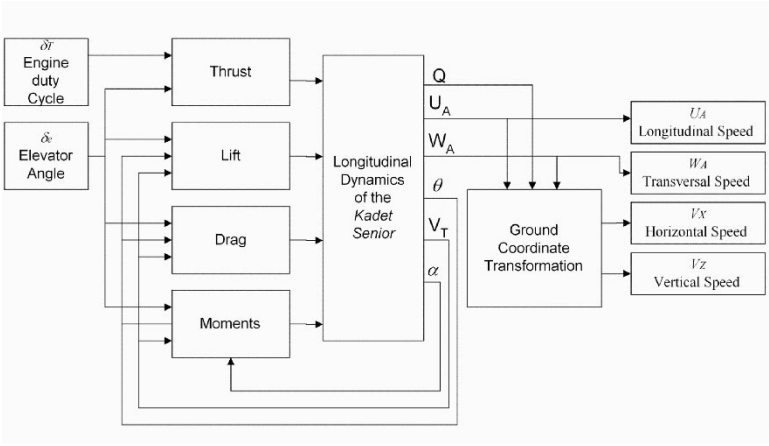

Fig. 6. Block diagram of the model.

appropriate parameters. These corrections were achieved by reducing the initial differences between the model and the real airplane.

Some noise and delay were added to the measured variables, simulating a real sensor, in order to make the model more authentic. The model response is an excellent approach to real airplane behavior. Therefore, it is useful to design and test control algorithms for the experimental platform. More details on this model are presented in the Appendix.

IV. Simulator Design and Control Strategy Tests

The purpose of the control strategy designed and tested in this section is to control airplane altitude and reduce oscillations

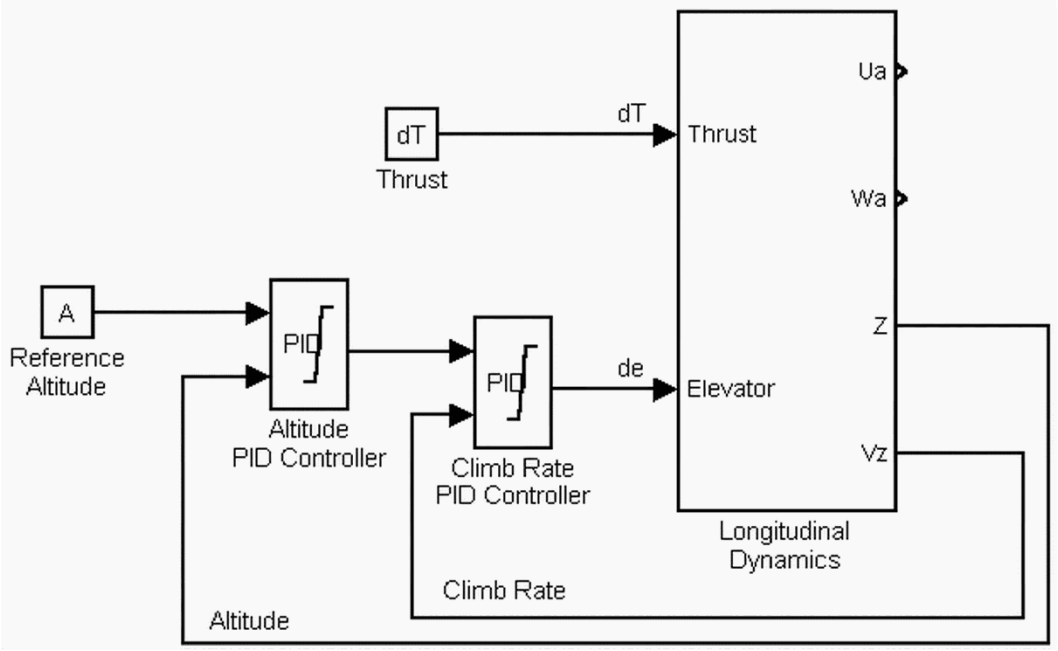

Fig. 7. Block diagram of the PID control strategy.

and stationary state errors using PID controllers. The block diagram for this control strategy (represented in Fig. 7) shows that the altitude controller acts on the elevator angle. The speed is open-loop controlled.

The altitude control strategy has two PID controllers in cascade (altitude and climb-rate controllers). This separation of controllers is possible because of the difference between the altitude time constants and the climb-rate control. The rise time for the altitude control depends on the difference between the initial and final altitude and has a typical value of 5 s in the tests performed for this paper; the climb-rate controller takes approximately 1 s to bring this variable to the set point.

The altitude controller inputs the altitude error and outputs the reference point for the climb-rate controller. This controller takes the difference between the estimated and the reference climb rate and generates a value for the elevator deflection δ_e.

This control system was tested by simulation using the model described in Section III. During the simulations, the parameters of the three PID controllers were calibrated by trial and error. Control system response, shown in Fig. 8, for a zero-delay, zero-noise model, and in Fig. 9, for a 0.1-s delay and noisy model.

The double-loop controller for the altitude responds quickly and smoothly (as shown in Fig. 8). Fig. 9 shows system sensitivity to noise in altitude measurements and a 0.1-s delay in the loop. Recalibration of the controllers improved their performance. Finally, a 3.3-s rise time and a 4-m overshoot were obtained.

The functionality of the same control strategy shown in the block diagram of Fig. 7, tuned for a noisy model, was tested in the experimental platform before using it as a demonstrator. Because of the similarity of the corrected mathematical model and the real airplane's behavior, the real airplane controllers (shown in Fig. 10) performed as well as expected (Fig. 9), so that fine-tuning was unnecessary. In this case, the rise time was as low as 1.1 s, and the overshoot did not reach 4 m (80% of

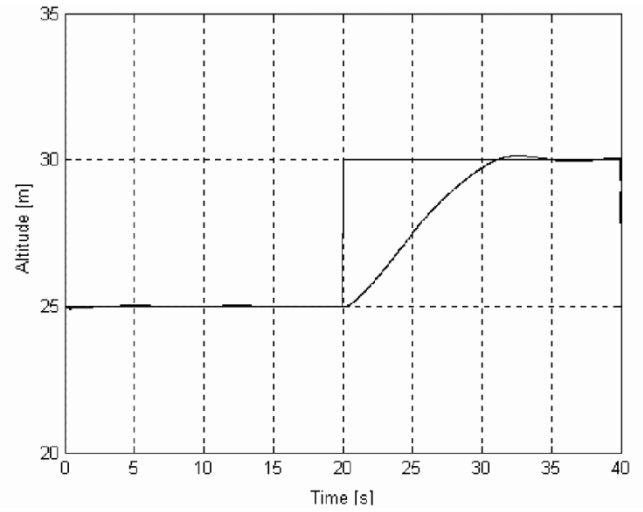

Fig. 8. Simulated altitude control in a zero-noise, zero-delay model.

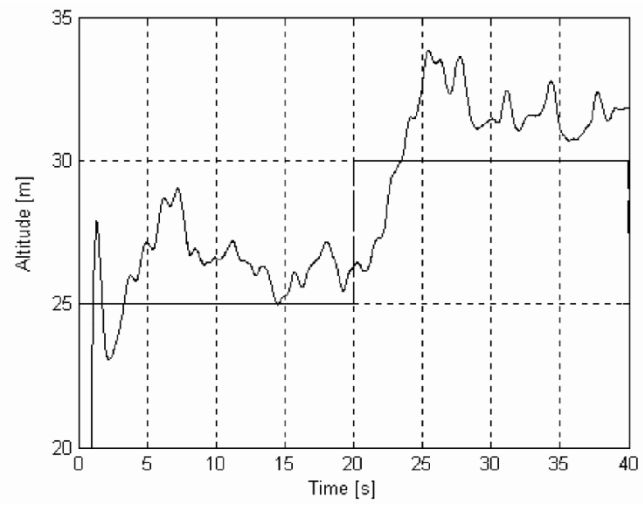

Fig. 9. Simulated altitude control in a noisy 0.1-s delay model.

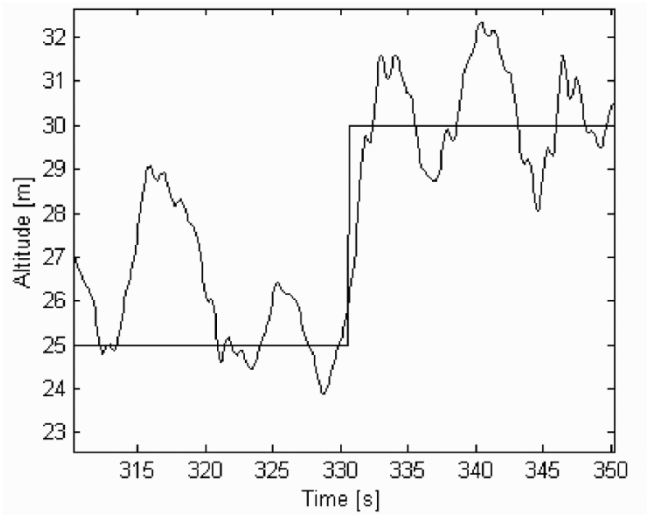

Fig. 10. Altitude control for the real airplane.

step); both performance indexes are comparable to the indexes obtained from simulations.

Two conclusions can be derived from the simulation tests. First, the experimental platform works properly for testing a particular control strategy. Second, the performance of the control strategy tested in this section is of sufficient quality to keep the altitude near the reference point. During the controlled flights, the control strategy worked safely, making manual control of the airplane unnecessary.

V. Application in an Automatic Control Course

The experimental platform was used to improve automatic control education in the course "IEE2612 Automatic Control" for undergraduate electrical engineering students at the Pontificia Universidad Católica de Chile (Chile's Pontifical Catholic University), Santiago; at that time, there were 106 students in the course. This section describes how the experiment was presented to the class, students' work, and discussions about the system.

A. First Presentation

During one of the first classes, the project was presented to the students. This presentation consisted basically of the development of the mathematical model, the sensors, the communications and acquisition systems, and the overall design, viewed as a real control problem example. The presentation continued with the design and tuning of the control strategies and the video projection of actual system tests. The objective was not to teach the students how to model and implement a real control system for an airplane but to introduce them to a real-life control problem and stir their interest in the project.

Students were very impressed with the presentation. Most comments were along the lines of "It's incredible that all these theoretical issues can be applied to a real system." Some of them asked about the sensors and other design problems, showing enthusiasm for the hardware and control algorithms. They also had time to discuss the importance of the mathematical model in designing a control system. Similar discussions about the sensors, the A/D converters, and their impact on system performance led the students to conclusions about the system's sensitivity to changes in the airplane, the sampling time, and the measurements.

B. Homework

When the students understood control systems and their behavior, they were asked to work with a Simulink model of the airplane to obtain an altitude controller. They were highly motivated because the best controllers would be used to control the real airplane in a public demonstration. The homework had three parts—open-loop simulations, design and tuning of a PID controller, and closed-loop simulations.

1) Open-Loop Simulations: Students were asked to simulate airplane behavior for predetermined manipulated variables and initial conditions. They were also asked to explain airplane behavior in terms of energy and intuitive knowledge of aerodynamic forces. In response, most explained that the airplane's aerodynamic forces (i.e., lift and drag) increase with speed. When speed increases, lift increases; and the airplane tends to increase its vertical speed, causing the pitch angle to increase and the airplane to head up. After a while, it gains potential energy and thereby loses speed and lift. This loss makes its nose drop; the plane loses altitude and increases its speed, thus starting the cycle again. This intuitive explanation matches the theoretical and simulated airplane behavior.

2) Design and Tuning of a PID Controller: Students were asked to design a PID controller for the airplane climb rate using a continuous-time, zero-noise model. Given the objective of introducing students to a real-life problem, the instructors asked students to assume that the airplane mathematical model was unknown; instead of using an analytical method, they would be forced to apply the Ziegler–Nichols method to tune the controller. To do so, students had to find the critic gain K_c for the climb-rate proportional controller and the oscillations period T_c using the model simulator. With these parameters and application of the Ziegler–Nichols formulas (1), they were able to find all the controller parameters, as follows:

$$K_P = 0.6K_c, \quad T_i = 0.5T_c, \quad T_d = 0.125T_c. \tag{1}$$

After designing the controller, students were asked to improve it by fine-tuning its parameters with several simulation trials. The final objective was to reduce the rms error of the altitude.

3) Closed-Loop Simulations: Students were asked to test their controller using a discrete-time noisy model similar to the real system. The altitude set point was given; they only had to change the controller block in the Simulink model. Because they used a discrete-time model with a slow sampling time, the results were not as good as they expected. With these results, they were able to reach conclusions about the importance of sampling time to system behavior. Fig. 11 shows the simulation results of the best controller in the class, tuned by one of the students.

C. Final Tests

The best three controllers were tested on the real airplane. To test a particular controller, it was enough to change the controller block (or parameters) in the Simulink model. Real test

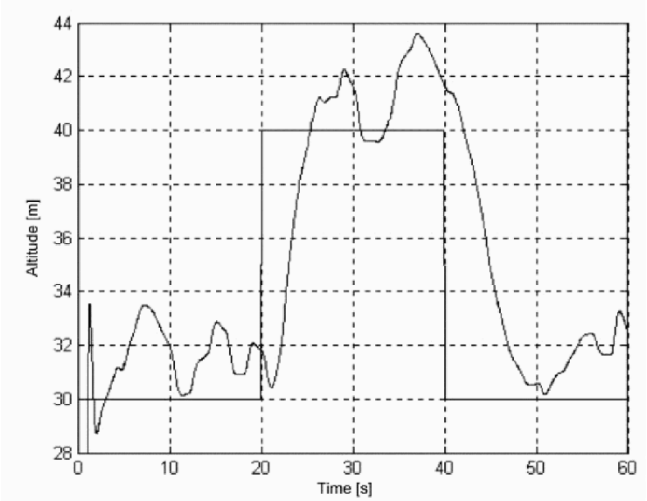

Fig. 11. Simulated altitude control in a noisy 0.1-s delay model performed by a student.

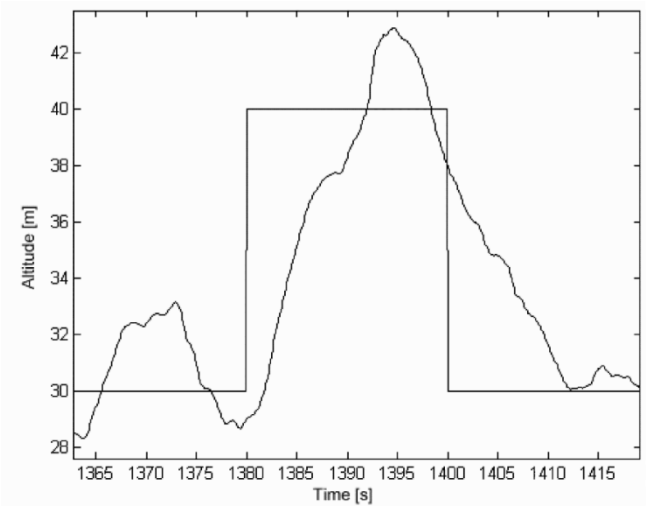

Fig. 12. Altitude control for the real airplane using a student-designed controller.

results (shown in Fig. 12) show the performance of the student-designed controllers and similarities between airplane behavior and the mathematical model (compared to Fig. 11). In the simulated case, the rise time is almost 5 s, and the overshoot reaches almost 2.3 m (23%); the experimental case presents a rise time of 11.5 s, and an overshoot of 3.1 m (31%). The differences observed between the two cases result from different initial states in the tests and wind gust disturbances in the experimental case. However, both results are comparable.

All students were invited to the presentation, but not all could attend because of other exams. Those who did were impressed by the computer's ability to control airplane altitude. They also showed great interest in the real-time measurement system for the airplane altitude.

D. Students' Appreciation of This Experience

As an important part of the project, students were asked to answer some questions about their experience with the airplane, rating it on a scale of 0 (worst) to 10 (best), with the following results:

- Automatic control topics applied in homework: 7.3;
- Topics learned while doing homework: 6.7;
- Motivation to do homework: 7.7;
- Homework's contribution to the course: 7.6;
- Homework's applicability to a real problem: 8;
- General appreciation of homework: 8.

This survey shows that overall students were satisfied with this work. They agreed that the homework contributed to course development; they realized the importance of working on a real problem for their education as engineers and appreciated the difficulties involved in working with real sensors and nonideal systems.

Most of the students agreed that the homework was motivating and interesting, but they would have liked to understand the model completely before working on it. They also encouraged the lecturers to keep working on this project and to try to apply this experience in other courses.

VI. Conclusion

Several conclusions can be reached from this paper. First, the objective of improving education in automatic control for undergraduate electrical engineering students was successfully met. Students were pleased to apply their knowledge to a real problem and learned and enjoyed developing their homework. In addition to the airplane's impact as a demonstrator, the students had another incentive: designing the best controller to have the honor of testing it using the real airplane.

Regarding the performance of this low-cost experimental platform, it is good enough to use as a base platform for teaching basic control systems. The altitude sensor and the communication system worked properly; however, better results can be obtained if delay times are reduced or a climb-rate sensor is added to obtain cleaner signals for this variable.

The mathematical model proved to be appropriate to test different control strategies for this platform. In fact, the controllers that work in simulations also work in the real airplane. Many of the model parameters needed to be corrected to improve the model quality.

The control system has proven to be of sufficient quality to control the airplane without needing any attitude or inertial sensors. This feature makes it possible to build low-cost altitude control systems with only pressure sensors.

On the other hand, some problems did arise during this experience. This system is difficult to test and demonstrate. It takes 45 min (or more) to set up the demonstration; its performance depends on the weather conditions (windy or rainy days are not suitable for testing the system). Finally, the demonstration requires the supervision of a qualified pilot for RC airplanes, and minimal security standards must be respected to avoid dangerous situations.

Finally, the idea of improving education by simulating a process and comparing its behavior with the real system is a teaching methodology that can be used in several courses; all that is needed is the designing of a teaching device (high-impact demonstrator) and using it to enrich the learning process.

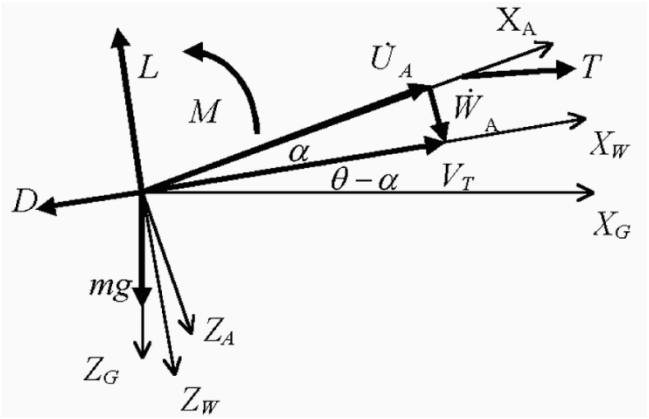

Fig. 13. Model reference systems.

In the future, this experience can be improved by enhancing the platform capabilities, adding more sensors and degrees of freedom. It can also be used to test and teach advanced control algorithms [4], [7], [8].

APPENDIX
MODEL SIMULATOR DETAILS

A. Basic Aerodynamics

The flight of any airplane is governed by four basic forces: the thrust (T), the weight (mg), the lift (L), and the drag (D). The first one is generated by the airplane engine and is related to its axis system. The second force is adapted to the earth coordinate system. The last ones, based on aerodynamics, are adapted to the reference system defined by the airplane velocity related to the wind V_T. These three reference systems are shown in Fig. 13, which also indicates the most important variables. The angle of attack α is defined as the angle between the airplane and the relative wind; the pitch angle θ is the angle between the aircraft and the ground. The airplane velocity related to the wind can be expressed in terms of the longitudinal speed $(\dot{U})$ and the vertical speed or climb rate $(\dot{W})$. All the aerodynamic forces are governed according to Bernoulli's principle and can be expressed as [3], [5]

$$F = C_F \cdot \frac{\rho \cdot V_T^2}{2} S \tag{2}$$

where C_F is a dimensionless coefficient for the force F, usually a nonlinear function of the angle of attack, Mach and Reynolds numbers, *downwash* angle and the action of some control surface, although it depends mostly on the shape of the airfoil; ρ is the air density; V_T is the airplane air speed; and S is the surface on which the force acts. This equation is used to calculate every aerodynamic force. The parameter S is always the wing surface, independent of the surface considered. For this reason, to calculate the forces acting on other surfaces, it is necessary to scale the force coefficients. The force coefficient for the entire airplane is the sum of all force coefficients for each part, weighted to obtain an appropriate value.

The moments acting on any surface are calculated around a fixed point, as the moment arm multiplied by the force equation, as follows:

$$M = C_M \cdot \frac{\rho \cdot V_T^2}{2} S \cdot c. \tag{3}$$

As a convention, the arm always takes the value of the mean aerodynamic chord (MAC) c, defined for the airplane main wing. In the Kadet Senior (a right-wing airplane), c equals the wing width. Since the coefficients used to calculate the forces and moments are dimensionless, these can be used for every wing with the same airfoil and different sizes. There are tables that specify the coefficients for every available airfoil so that those designers can do their calculations based on experience.

B. Generalized Aircraft Model

The mathematical model that describes the longitudinal dynamics of an airplane is defined using the equations derived from Newton's second law [3], [5]

$$\sum F_X = m \cdot (\dot{U}_A + W_A Q) \tag{4}$$

$$\sum F_Z = m \cdot (\dot{W}_A - U_A Q) \tag{5}$$

and

$$\sum M_Y = I_Y \cdot \dot{Q}. \tag{6}$$

In the previous equations, three of the six degrees of freedom of the airplane movement have been omitted, and it has been assumed that the mass (m) and the moment of inertia (I_Y) are constant and that the plane XZ of the airplane is a plane of symmetry. Therefore, forces and moments can be expressed as

$$\sum F_X = T\cos(\alpha_T) + L\sin(\alpha) - D\cos(\alpha) - mg\sin(\theta) \tag{7}$$

$$\sum F_Z = T\sin(\alpha_T) - L\cos(\alpha) - D\sin(\alpha) + mg\cos(\theta) \tag{8}$$

and

$$\sum M_Y = M_T + M_w + M_t + M_{\dot{\alpha}}. \tag{9}$$

The parameter α_T defines the angle between the thrust and the airplane axis system. There are four moments: M_T for the thrust, M_w for the wing, M_t for the tail, and $M_{\dot{\alpha}\dot{\theta}}$, which appears when α or θ changes. Each force and moment shown in (7), (8), and (9) will be analyzed.

1) Forces and Moments on the Airplane: Thrust depends on δ_T and other factors, such as altitude and air speed, according to the engine type used [3]. It can be obtained as

$$T = f(V_T, h, \delta_T, \ldots). \tag{10}$$

The Kadet Senior is propelled by a fixed-blade propeller, generating a force that decreases linearly with the speed and can be expressed as

$$T = (T_0 + C_{TV} \cdot V_T) \cdot \delta_T \tag{11}$$

where T_0 is the maximum force of the system, and C_{TV} is the decrease rate of the force with respect to the speed; C_{TV}

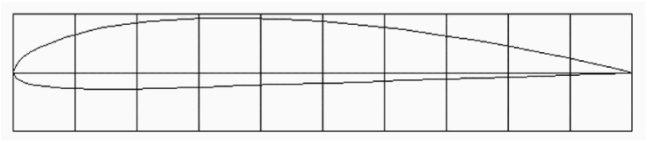

Fig. 14. Clark-Y airfoil.

has a negative value. Both parameters can be experimentally obtained.

Before analyzing all the aerodynamic forces involved in airplane motion, it is necessary to study the *downwash* effect. This effect takes place as a result of the airflow between the lower and the upper surfaces of the wing. This vertical flow disturbs the horizontal airflow and produces a decrease in the effective angle of attack on the airplane tail according to the following equation:

$$\alpha_t(\alpha, \varepsilon, \delta_e) = \alpha + i - \varepsilon + \tau \cdot \delta_e. \tag{12}$$

In (12), i is the fixed angle between the wing and tail chords, which is zero in the Kadet Senior; ε is the *downwash* angle, which can be modeled in several ways; δ_e is the elevator angle, positive when the elevator is down; and τ is the effectiveness of the elevator, which has a value of 0.15 in the Kadet Senior. This information is obtained from charts of the elevator to horizontal stabilizer surface ratio [9]. The numerical expression for the *downwash* angle as a function of the angle of attack in radians is obtained as [10]

$$\varepsilon(\alpha) = 0.0916 C_{\mathrm{Lw}}(\alpha) + 0.00436. \tag{13}$$

Using the previous equation, it is possible to calculate the aerodynamic forces for the entire airplane.

The total *lift* is constituted by the lift generated in the wing, the tail, and the fuselage. In the Kadet Senior, the wing is the most important source of lift; on the other hand, the fuselage generates a small lift, very difficult to model, that will be neglected in this work. Thus, calculating the lift coefficient for the entire airplane considers the wings and the tail, as follows:

$$C_L = C_{\mathrm{Lw}} + k \cdot C_{\mathrm{Lt}}. \tag{14}$$

The wing-lift coefficient is obtained from charts and graphics derived from wind tunnel tests for the used airfoil; the tail-lift coefficient is obtained in the same way, but it has to be weighted to fit in (2). Constant k is a coefficient that considers the surfaces of the wing and horizontal stabilizer. Then, the entire airplane lift coefficient is [9]

$$C_L(\alpha, \delta_e) = C_{\mathrm{Lw}}(\alpha) + \frac{S_t}{S}\eta_t C_{\mathrm{Lt}}\big(\alpha_t(\alpha, \delta_e)\big) \tag{15}$$

where S_t is the horizontal stabilizer surface and η_t is tail efficiency.

The Kadet Senior wing is based on a Clark-Y-type airfoil, shown in Fig. 14. The lift coefficient of this airfoil can be plotted as a function of the angle of attack for low Mach numbers, as shown in Fig. 15. One can see that the lift coefficient presents a fall for angles greater than 15°. This fact is a result of the vorticity effect, called *stall*, that appears in the superior surface of the wing and tends to reduce the airplane lift. Two straight lines connected with an arctangent function approached the lift

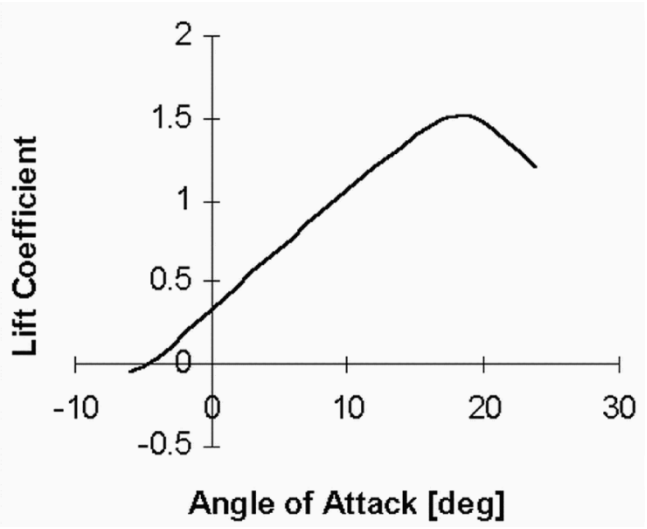

Fig. 15. Lift coefficient for Clark-Y airfoil.

coefficient curve for the wing. The tail-lift coefficient curve was fitted to a straight line. Using the numerical expressions for both coefficients and replacing their values in (15), total airplane lift can be expressed as

$$L = C_L(\alpha, \delta_e)\frac{\rho \cdot V_T^2}{2}S. \tag{16}$$

The *drag* calculation for the entire airplane is similar to the lift calculation. First, it is necessary to calculate the drag coefficient for the entire airplane, adding the weighted drag coefficients of each part, as follows:

$$C_D = C_{\mathrm{Dw}} + k \cdot C_{\mathrm{Dt}}. \tag{17}$$

As in the lift case, (17) can be written in extended form

$$C_D(\alpha, \delta_e) = C_{\mathrm{Dw}}(\alpha) + \frac{S_t}{S}\eta_t C_{\mathrm{Dt}}(\alpha_t(\alpha, \delta_e)). \tag{18}$$

The drag coefficients of the tail and wing can be obtained from charts. These coefficients have a parabolic shape as a function of the angle of attack and can be approximated to a second-order Taylor series. Replacing these values in (18), the total drag coefficient C_D is obtained. The total airplane drag can be obtained by replacing this coefficient in (2), as follows:

$$D = C_D(\alpha, \delta_e)\frac{\rho \cdot V_T^2}{2}S. \tag{19}$$

The *moments* acting on the airplane are considered around its center of gravity (c.o.g.) so that the weight does not contribute. Moments can be generated in the engine, wing, tail, and fuselage, although this last one will not be calculated in this paper because of its small contribution and the difficulty of modeling it in analytic form. An important moment-generating source is the airplane elevator. The generated moment included in the tail moment equation allows controlling the pitch angle.

The thrust moment is calculated as the cross product of the propulsion and its arm. In the case of the Kadet Senior, the arm of this moment is too small and can be excluded from the model.

The airplane's aerodynamic moments exist as a result of the forces acting in its aerodynamic center (a.c.), which is not necessarily the c.o.g. The relative position between both defines

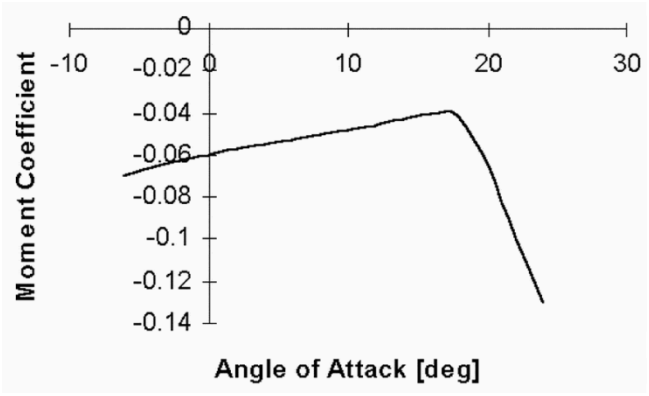

Fig. 16. Moment coefficient for *Clark-Y* airfoil.

the airplane stability. If the a.c. is ahead of the c.o.g., a small increase of the angle of attack tends to increase the moment, which makes the airplane unstable [5]. This situation means that the airplane wings are inherently unstable since they have the a.c. ahead of its c.o.g. In order to move their a.c. backward, airplanes have a tail that generates forces behind the c.o.g. In the next paragraphs, the tail and wing moments are determined.

Wing moment coefficients, for moments measured from the first quarter of the wing chord, appear in charts derived from wind tunnel tests. To calculate moments acting around the airplane c.o.g., it is necessary to add a component that includes the aerodynamic force produced by the wing. In this calculation, which follows, the drag force is usually neglected:

$$C_{\mathrm{Mw}}(\alpha) = C_{\mathrm{Mwac}}(\alpha) + \frac{x_w}{c} C_{\mathrm{Lw}}(\alpha). \tag{20}$$

In (20), the term x_w is the arm of the moment caused by the wing lift; it has a positive value if the wing a.c. is ahead of the airplane c.o.g. The term C_{Mwac} is plotted in Fig. 16. Through a regression in the linear range $-5^\circ < \alpha < 15^\circ$, it is possible to obtain a first-order function for that moment coefficient; for more precision in the model, higher order functions are recommended.

Tail moments are calculated as the arm multiplied by the tail lift and weighted to be included in the general equation of moments [9], as follows:

$$C_{\mathrm{Mt}}(\alpha_t, \delta_e) = \frac{x_t S_t}{cS} \eta_t C_{\mathrm{Lt}}(\alpha_t, \delta_e). \tag{21}$$

The term x_t is the moment arm (negative) and tends to stabilize the airplane. In this equation, the term C_{Lt} grows linearly with the angle of attack of the tail, which depends on the elevator angle δ_e [(12)]. Thus, the elevator angle directly controls the total airplane moment.

There are other moments in the flight of the airplane, which appear because of changes in the attack or pitch angles. These moments reduce transient response oscillations but are difficult to model analytically. In this paper, their coefficients will be modeled as linear functions of change in the angle of attack and pitch angle. The equation for these coefficients is, therefore,

$$C_{M\dot{\alpha}\dot{\theta}}(\dot{\alpha}, \dot{\theta}) = C_{M\dot{\alpha}} \cdot \dot{\alpha} + C_{M\dot{\theta}} \cdot (\dot{\theta} - \dot{\alpha}) \tag{22}$$

where $C_{M\dot{\alpha}}$ and $C_{M\dot{\theta}}$ are chosen to minimize the differences between the simulated and the real airplane behavior. The moment coefficients are applied to (14), obtaining the following expression for the total moment:

$$M = \left(C_{\mathrm{Mw}}(\alpha) + C_{\mathrm{Mt}}(\alpha_t, \delta_e) + C_{M\dot{\alpha}\dot{\theta}}(\dot{\alpha}, \dot{\theta})\right) \frac{\rho V_T^2 S}{2} c. \tag{23}$$

TABLE I
STRUCTURAL PARAMETERS OF THE *KADET SENIOR*

Parameter	Value	Unit
Total mass m	6	kg
Moment of inertia around the c. o. g. I_y	1.233	kgm^2
Wing surface S	0.742	m^2
Horizontal stabilizer surface S_t	0.2	m^2
Mean aerodynamic chord c	0.37	m
Wing aerodynamic center x_w	0.02	m
Tail aerodynamic center x_t	-0.82	m
Angle between thrust and airplane axis α_t	-9.3E-2	rad
Thrust arm x_{thrust}	neglected	-
Elevator effectiveness τ	0.15	-
Tail efficiency η_t	0.8	-

TABLE II
EXTERNAL PARAMETERS REQUIRED FOR SIMULATION

Parameter	Value	Unit
Acceleration of gravity g	9.8	m/s^2
Air density ρ	1.2	kg/m^3

C. Application to the RC Kadet Senior

Some of the parameters required to program this model airplane have been described previously. Others, from airplane plans, are shown in Table I. External parameters required for simulation are presented in Table II.

D. Flight Simulation Programming

Before simulating airplane behavior, one must define the mathematical model's inputs and outputs. The inputs are the engine duty cycle and the elevator angle.

Engine duty cycle δ_T is a dimensionless magnitude that is limited to between 0 and 1 and represents the manipulated variable that defines the engine force.

Elevator angle δ_e is the magnitude that defines the angle between the elevator and the horizontal stabilizer. It is limited between -0.5 rad (elevators up) and 0.5 rad (elevators down).

The model outputs airplane longitudinal U_A and transversal speed W_A in its own coordinate system; these variables can be obtained by integrating the accelerations. By means of coordinate change and a second integration, one can obtain the airplane altitude z_G as follows:

$$z_G = \int \left(U_A \sin(\theta) - W_A \cos(\theta)\right) dt. \tag{24}$$

Other relationships are important to programming the simulation to obtain the internal variables

$$V_T = \sqrt{U_A^2 + W_A^2} \tag{25}$$

$$\alpha = \operatorname{atan}\left(\frac{W_A}{U_A}\right) \tag{26}$$

and

$$\dot{\theta} = Q. \tag{27}$$

ACKNOWLEDGMENT

The authors wish to thank the IEE2612 students for evaluating and cooperating with this activity.

REFERENCES

[1] T. H. Wong, "Design of a magnetic levitation control system—An undergraduate project," *IEEE Trans. Educ.*, vol. E-29, Nov. 1986.
[2] W. G. Hurley and W. H. Wölfle, "Electromagnetic design of a magnetic suspension system," *IEEE Trans. Educ.*, vol. 40, May 1997.
[3] J. Blakelock, *Automatic Control of Aircraft and Missiles*, 2nd ed. New York: Wiley, 1991, ch. 1.
[4] E. F. Camacho and C. Bordons, *Model Predictive Control*. New York: Springer-Verlag, 1999, ch. 1–4.
[5] D. McRuer, I. Ashkenas, and D. Graham, *Aircraft Dynamics and Automatic Control*. Princeton, NJ: Princeton Univ. Press, 1973, ch. 5.
[6] E. A. Morelli, "Global nonlinear parametric modeling with application to F-16 aerodynamics," presented at the American Control Conf., Philadelphia, PA, June 24–28, 1998.
[7] R. Palm and D. Driankov, *Model Based Fuzzy Control*. New York: Springer-Verlag, 1997, ch. 1.
[8] S. Skogestad and I. Postlethwaite, *Multivariable Feedback Control: Analysis and Design*. New York: Wiley, 1996, ch. 1–3.
[9] R. Nelson, *Flight Stability and Automatic Control*. Columbus, OH: McGraw-Hill, 1997, ch. 1–4.
[10] ——, (1998) Model Airplanes Radio Control R/C Website. [Online]. Available: http://www.geocities.com/CapeCanaveral/Hangar/6875/downwash.html

Angel Abusleme (M'01) received the electrical engineering and the M.Sc. degrees in automatic control from the Pontificia Universidad Católica de Chile, Santiago, in 2000.

Since 2001, he has been an Instructor in the Electrical Engineering Department, Pontificia Universidad Católica de Chile. His main research interests are unmanned air vehicles and electrodynamic suspension systems.

Aldo Cipriano (S'78–M'78–SM'95) received the electrical engineering and the Master degrees from the University of Chile, Santiago, and the Dr. Ing. degree from the Technical University of Munich, Munich, Germany, in 1973, 1974, and 1981, respectively.

Currently, he is the Dean of the College of Engineering and Professor of the Electrical Engineering Department, Pontificia Universidad Católica de Chile, Santiago. He has worked as a consultant in Chile and Argentina. His main research interests are in the areas of control and industrial automation. He has led several R&D projects in these areas.

Dr. Cipriano is a past President of the Chilean Automatic Control Society (ACCA).

Marcello Guarini received the electrical engineering degree from the Pontificia Universidad Católica de Chile, Santiago, and the M.Sc. and Ph.D. degrees from the University of Arizona, Tucson, in 1976, 1983, and 1989, respectively.

He is Professor of the Electrical Engineering Department of the Pontificia Universidad Católica de Chile. His main current research interests are in modeling, simulation and parameter estimation of the cardiovascular system, and the development of spectral-based numerical methods. He also works in vision-based industrial instrumentation for the local industry. He has led several research projects in these areas.

Dr. Guarini is Member of the Chilean Automatic Control Society (ACCA) and of the Society for Computer Simulation International (SCS International).